Analysis of Shear Waves in Bonded Layers Using Springs Model

Mihai Valentin Predoi, Latifa Attar, Ech-Cherif Mounsif El Kettani, Damien Leduc, Pascal Pareige

Analysis of Shear Waves in Bonded Layers Using Springs Model

Mihai Valentin PREDOI
Department of Mechanics, University Politehnica of Bucharest, Splaiul Independentei 313, 060042 Bucharest, Romania, predoi@cat.mec.pub.ro

Latifa ATTAR
LOMC UMR CNRS 6294, University of Le Havre, 75 rue Bellot, 76600 Le Havre, France, latifa.attar@gmail.com

Mounsif Ech-Cherif EL-KETTANI
LOMC UMR CNRS 6294, University of Le Havre, 75 rue Bellot, 76600 Le Havre, France, mounsif.elkettani@univ-lehavre.fr

Damien LEDUC
LOMC UMR CNRS 6294, University of Le Havre, 75 rue Bellot, 76600 Le Havre, France, damien.leduc@univ-lehavre.fr

Pascal PAREIGE
LOMC UMR CNRS 6294, University of Le Havre, 75 rue Bellot, 76600 Le Havre, France, pascal.pareige@univ-lehavre.fr

Abstract: - Bonding is a widely used technique especially for composite assemblies. The quality of bonding depends on many parameters. The bonding strength is a global and one of the most important parameters in bonding quality assessment. Guided ultrasonic waves have been used in the last decades to assess the bond quality, or by detecting a weak adhesion, cracks, etc. Guided waves require a well-adapted mathematical and numerical model to simulate the measurable parameters in the real case. Among these models, the elastic interface represented by a distribution of springs, was used to model the whole adhesive layer or only the contact between layers. Weaker spring constants can represent local adhesion degradation. In the present paper we investigate the applicability limits of this model in the particular case of shear-horizontal (SH) waves.

Keywords: - bonding, shear-horizontal waves, spring model

1. INTRODUCTION

Bonding strength depends not only on the cohesive properties of the adhesive but also on the adhesive properties at the contact surfaces between the adhesive and the bonded surfaces. The simplest model for the adhesion is a distribution of massless linear-elastic springs. This model was introduced, to the authors knowledge by Jones and Whittier [1] in 1967. The model was used as interface model for shear horizontal (SH) waves [2] and for Lamb waves: Lowe et al. [3] Heller et al, [4] Hosten and Castaings [5] Gauthier et al. [6].

In the present work, a detailed presentation of the SH modes in single layer, two-layers and three-layers has a didactic purpose. The spring interphase is investigated, providing intervals of adequate characterization of the adhesive properties. The influence of change in spring's forces signs on the dispersion curves and modal shapes is also discussed.

2. THEORETICAL ASPECTS

The main hypothesis concerning the SH waves is the modal displacement field ($U=V=0$, $W(y)$) shown on Figure 1. The motion is defined by $w(x,y,t)=W(y)\exp\left[i(kx-\omega t)\right]$, but the harmonic factor $\exp\left[i(kx-\omega t)\right]$ will be omitted in the following. Plane wave hypothesis implies $\frac{\partial \bullet}{\partial z}\equiv 0$. The usual notations are used: k for the wavenumber of the SH waves and $\omega=2\pi f$, is the angular frequency, corresponding to the frequency f. The dynamic elasticity equations valid for the SH guided waves can be deduced for orthotropic materials:

$$-k^2 C_{55} W + \frac{\partial}{\partial y}\left[C_{44}\frac{\partial W}{\partial y}\right] = -\rho\omega^2 W \ . \qquad (1)$$

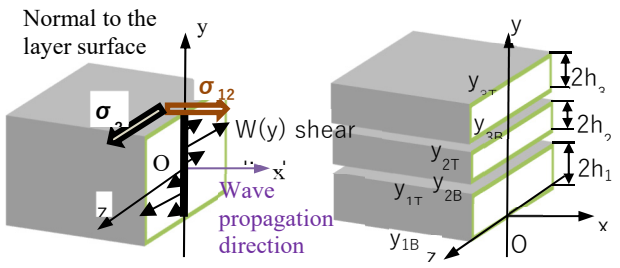

Figure 1. Displacement field and stress components involved in the SH waves propagation (left) and an example of three layered lamina (right).

Assuming C_{44} to be constant in each layer, this differential equation, has the general solution:

$$W(y) = A\cos(\alpha y) + B\sin(\alpha y). \tag{2}$$

The notation $\alpha = \sqrt{\dfrac{\rho\omega^2 - k^2 C_{55}}{C_{44}}}$ was used.

For an orthotropic material, with the indicated axes, the Cauchy stress tensor components are denoted:

$$\begin{pmatrix} S_{11} \\ S_{22} \\ S_{33} \\ S_{23} \\ S_{13} \\ S_{12} \end{pmatrix} = \begin{pmatrix} C_{11} & C_{12} & C_{13} & 0 & 0 & 0 \\ C_{12} & C_{22} & C_{23} & 0 & 0 & 0 \\ C_{13} & C_{23} & C_{33} & 0 & 0 & 0 \\ 0 & 0 & 0 & C_{44} & 0 & 0 \\ 0 & 0 & 0 & 0 & C_{55} & 0 \\ 0 & 0 & 0 & 0 & 0 & C_{66} \end{pmatrix} \begin{pmatrix} 0 \\ 0 \\ 0 \\ \dfrac{\partial W}{\partial y} \\ ikW \\ 0 \end{pmatrix}$$

There are two stress components, one is always null ($\sigma_{12} \equiv 0$) and the other is denoted σ_{23}, as shown on Figure 1, for the upper and lower surfaces of the lamina. The stress components σ_{23} cancel if the surfaces are free:

$$\sigma_{23} = C_{44}\frac{\partial W}{\partial y} = 0. \tag{3}$$

We consider two and three layers of constant thickness in contact, one of these layers representing the adhesive. The simplest mathematical case represents the perfect contact between elastic layers. In this care, there is continuity of displacement and stress σ_{23}, meaning continuity of shear displacement W and its derivative $\dfrac{\partial W}{\partial y}$, between layers.

In reality there is a transition of elastic properties in the bond layer, especially at the contact with the bonded surfaces. This transition of adhesive properties depends on the manufacturing conditions (temperature, surface roughness, applied pressure and cure time). The global bonding strength depends to a great extent, on the adhesive properties in these very thin transition layers.

One method used to model the transition in these thin layers, is to introduce between the bonded layers and the adhesive layer, a jump of displacements as boundary condition, generating shear stresses in a uniform distribution of springs:

$$\sigma_{23} = R_S\left(W_{up} - W_{down}\right) \tag{4}$$

in which W_{up} and W_{down} represent the shear displacements on the upper layer and respectively the lower layer involved in the bonding.

The transition layer thickness is not a parameter of this model. This represents the so-called model of Jones [1]. It can be noted that the shear stress (4) is positive or negative according to the choice of the term's order in the difference. In the following, some limitations of this model are investigated.

2.1. A single layer

We consider a single elastic layer of constant thickness $y_{1T} - y_{1B} = 2h_1$, denoted by an upper index $^{(1)}$, as shown on Figure 1b. The boundary conditions can be written for y_{1B} and y_{1T} either for displacements, or for stresses:

$$\begin{aligned} W_B^{(1)} &= A_1\cos\left(\alpha^{(1)}y_{1B}\right) + B_1\sin\left(\alpha^{(1)}y_{1B}\right) \\ S_{23B}^{(1)} &= C_{44}^{(1)}\alpha^{(1)}\left[-A_1\sin\left(\alpha^{(1)}y_{1B}\right) + B_1\cos\left(\alpha^{(1)}y_{1B}\right)\right] \\ W_T^{(1)} &= A_1\cos\left(\alpha^{(1)}y_{1T}\right) + B_1\sin\left(\alpha^{(1)}y_{1T}\right) \\ S_{23T}^{(1)} &= C_{44}^{(1)}\alpha^{(1)}\left[-A_1\sin\left(\alpha^{(1)}y_{1T}\right) + B_1\cos\left(\alpha^{(1)}y_{1T}\right)\right] \end{aligned} \tag{5}$$

If the displacements are imposed on the bottom $W_B^{(1)}$ or top $W_T^{(1)}$ surfaces, then the first and third equations from the system (5) will represent the boundary conditions providing the dispersion equation. In most practical cases however, stress free surfaces are considered, so that the second and fourth equations provide the dispersion equation:

$$\begin{vmatrix} -\sin\left(\alpha^{(1)}y_{1B}\right) & \cos\left(\alpha^{(1)}y_{1B}\right) \\ -\sin\left(\alpha^{(1)}y_{1T}\right) & \cos\left(\alpha^{(1)}y_{1T}\right) \end{vmatrix} = 0. \tag{6}$$

2.2. Two layers in perfect contact

A second layer, indicated by upper index $^{(2)}$, will have similar boundary conditions as those defined by eq. (5). The perfect continuity at $y_{1T} = y_{2B} = y_L$ (see Figure 1b) of the shear displacement and stress fields means:

$$W_T^{(1)}(y_L) = W_B^{(2)}(y_L);\ S_{23T}^{(1)}(y_L) = S_{23B}^{(2)}(y_L). \qquad (7)$$

Consequently, the full set of possible boundary conditions can be cast into matrix form as:

$$\begin{bmatrix} c_{1B} & s_{1B} & 0 & 0 \\ -C_{44}^{(1)}\alpha^{(1)}\mathrm{s}_{1B} & C_{44}^{(1)}\alpha^{(1)}\mathrm{c}_{1B} & 0 & 0 \\ c_{IL} & s_{1L} & -c_{2L} & -s_{2L} \\ -C_{44}^{(1)}\alpha^{(1)}s_{1L} & C_{44}^{(1)}\alpha^{(1)}c_{1L} & C_{44}^{(2)}\alpha^{(2)}s_{2L} & -C_{44}^{(2)}\alpha^{(2)}\mathrm{c}_{2L} \\ 0 & 0 & c_{2T} & s_{2T} \\ 0 & 0 & -C_{44}^{(2)}\alpha^{(2)}s_{2T} & C_{44}^{(2)}\alpha^{(2)}\mathrm{c}_{2T} \end{bmatrix} \begin{bmatrix} A_1 \\ B_1 \\ A_2 \\ B_2 \end{bmatrix} = \begin{bmatrix} W_B^{(1)} \\ S_{23B}^{(1)} \\ 0 \\ 0 \\ W_T^{(2)} \\ S_{23T}^{(2)} \end{bmatrix}$$

The following notations are used for each of the two layers:

$$\alpha^{(i)} = \sqrt{\frac{\rho^{(i)}\omega^2 - k^2 C_{55}^{(i)}}{C_{44}^{(i)}}};\ i = 1,2;$$
$$s_{1B} = \sin\left(\alpha^{(1)} y_B\right);\ \ c_{1B} = \cos\left(\alpha^{(1)} y_H\right);$$
$$s_{1L} = \sin\left(\alpha^{(1)} y_L\right);\ \ c_{1L} = \sin\left(\alpha^{(1)} y_L\right);$$
$$s_{2L} = \sin\left(\alpha^{(2)} y_L\right);\ \ c_{2L} = \sin\left(\alpha^{(2)} y_L\right);$$
$$s_{2T} = \sin\left(\alpha^{(2)} y_{2T}\right);\ \ c_{2T} = \sin\left(\alpha^{(2)} y_{2T}\right);$$

The continuity conditions have been transformed into equations 3 and 4 of this system of equations. From the six equations, only four equations will be used, corresponding to the imposed boundary conditions at y_{1B} and y_{2T} respectively. The usual stress-free surfaces case, imply discarding the first and 5-th equations. The remaining 4 by 4 determinant represents the dispersion equation in this case:

$$\begin{vmatrix} -\mathrm{s}_{1B} & \mathrm{c}_{1B} & 0 & 0 \\ \mathrm{c}_{1L} & \mathrm{s}_{1L} & -\mathrm{c}_{2L} & -\mathrm{s}_{2L} \\ -\alpha^{(1)}/\alpha^{(2)}\,\mathrm{s}_{1L} & \alpha^{(1)}/\alpha^{(2)}\,\mathrm{c}_{1L} & C_{44}^{(2)}/C_{44}^{(1)}\,\mathrm{s}_{2L} & -C_{44}^{(2)}/C_{44}^{(1)}\,\mathrm{c}_{2L} \\ 0 & 0 & -s_{2T} & \mathrm{c}_{2T} \end{vmatrix} = 0 \qquad (8)$$

2.3. Two layers with springs interface

The spring interface between layers defined by equation can be written at the interface $y_{1T} = y_{2B} = y_L$ as:

$$S_{23T}^{(1)} = R_S^{(1)}\left(W_B^{(2)} - W_T^{(1)}\right) = C_{44}^{(1)}\alpha^{(1)}\left[-A_1\sin\left(\alpha^{(1)}y_L\right) + B_1\cos\left(\alpha^{(1)}y_L\right)\right]$$
$$S_{23L}^{(2)} = -R_S^{(1)}\left(W_B^{(2)} - W_T^{(1)}\right) = C_{44}^{(2)}\alpha^{(2)}\left[-A_2\sin\left(\alpha^{(2)}y_L\right) + B_2\cos\left(\alpha^{(2)}y_L\right)\right] \qquad (9)$$

Using these two equations for the interface, the set of possible boundary conditions becomes:

$$\begin{bmatrix} \mathrm{c}_{1B} & \mathrm{s}_{1B} & 0 & 0 \\ -C_{44}^{(1)}\alpha^{(1)}\mathrm{s}_{1B} & C_{44}^{(1)}\alpha^{(1)}\mathrm{c}_{1B} & 0 & 0 \\ csa_{1L} - R_S^{(1)}\mathrm{c}_{1L} & -cca_{1L} - R_S^{(1)}\mathrm{s}_{1L} & R_S^{(1)}\mathrm{c}_{2L} & R_S^{(1)}\mathrm{s}_{2L} \\ -R_S^{(1)}\mathrm{c}_{1L} & -R_S^{(1)}\mathrm{s}_{1L} & csa_{2L} + R_S^{(1)}\mathrm{c}_{2L} & -cca_{2L} + R_S^{(1)}\mathrm{s}_{2L} \\ 0 & 0 & \mathrm{c}_{2T} & \mathrm{s}_{2T} \\ 0 & 0 & -C_{44}^{(2)}\alpha^{(2)}\mathrm{s}_{2T} & C_{44}^{(2)}\alpha^{(2)}\mathrm{c}_{2T} \end{bmatrix} \begin{bmatrix} A_1 \\ B_1 \\ A_2 \\ B_2 \end{bmatrix} = \begin{bmatrix} W_B^{(1)} \\ S_{23B}^{(1)} \\ 0 \\ 0 \\ W_T^{(2)} \\ S_{23T}^{(2)} \end{bmatrix}$$

The following notations were used:

$$csa_{1L} = C_{44}^{(1)}\alpha^{(1)}\sin\left(\alpha^{(1)}y_L\right);\ \ cca_{1L} = C_{44}^{(1)}\alpha^{(1)}\cos\left(\alpha^{(1)}y_L\right);$$
$$csa_{2L} = C_{44}^{(2)}\alpha^{(2)}\sin\left(\alpha^{(2)}y_L\right);\ \ cca_{2L} = C_{44}^{(2)}\alpha^{(2)}\cos\left(\alpha^{(2)}y_L\right);$$

The dispersion equation written in the classical case of free surfaces becomes:

$$\begin{vmatrix} -\mathrm{s}_{1B} & \mathrm{c}_{1B} & 0 & 0 \\ csa_{1L} - R_S^{(1)}\mathrm{c}_{1L} & -cca_{1L} - R_S^{(1)}\mathrm{s}_{1L} & R_S^{(1)}\mathrm{c}_{2L} & R_S^{(1)}\mathrm{s}_{2L} \\ -R_S^{(1)}\mathrm{c}_{1L} & -R_S^{(1)}\mathrm{s}_{1L} & csa_{2L} + R_S^{(1)}\mathrm{c}_{2L} & -cca_{2L} + R_S^{(1)}\mathrm{s}_{2L} \\ 0 & 0 & -\mathrm{s}_{2T} & \mathrm{c}_{2T} \end{vmatrix} = 0 \qquad (10)$$

2.4. Three layers in perfect contact

A third layer indicated by upper index $^{(3)}$ is here considered (Figure 1). The perfect continuity at $y_{1T} = y_{2B} = y_L$ and at $y_{2T} = y_{3B} = y_H$ (see Figure 1b) of the displacement and stress fields, means:

$$\begin{aligned} W_T^{(1)}(y_L) &= W_B^{(2)}(y_L);\quad S_{23T}^{(1)}(y_L) = S_{23B}^{(2)}(y_L) \\ W_T^{(2)}(y_T) &= W_B^{(3)}(y_T);\quad S_{23T}^{(2)}(y_T) = S_{23B}^{(3)}(y_T). \end{aligned} \qquad (11)$$

The full set of boundary conditions in this case is:

$$\begin{bmatrix} \mathrm{c}_{1B} & \mathrm{s}_{1B} & 0 & 0 & 0 & 0 \\ -C_{44}^{(1)}\alpha^{(1)}\mathrm{s}_{1B} & C_{44}^{(1)}\alpha^{(1)}\mathrm{c}_{1B} & 0 & 0 & 0 & 0 \\ \mathrm{c}_{1L} & \mathrm{s}_{1L} & -\mathrm{c}_{2L} & -\mathrm{s}_{2L} & 0 & 0 \\ \frac{\alpha^{(1)}}{\alpha^{(2)}}\mathrm{s}_{1L} & \frac{\alpha^{(1)}}{\alpha^{(2)}}\mathrm{c}_{1L} & \frac{C_{44}^{(2)}}{C_{44}^{(1)}}\mathrm{s}_{2L} & \frac{C_{44}^{(2)}}{C_{44}^{(1)}}\mathrm{c}_{2L} & 0 & 0 \\ 0 & 0 & \mathrm{c}_{2H} & \mathrm{s}_{2H} & -\mathrm{c}_{3H} & -\mathrm{s}_{3H} \\ 0 & 0 & \frac{\alpha^{(2)}}{\alpha^{(3)}}\mathrm{s}_{2H} & \frac{\alpha^{(2)}}{\alpha^{(3)}}\mathrm{c}_{2H} & \frac{C_{44}^{(3)}}{C_{44}^{(2)}}\mathrm{s}_{3H} & \frac{C_{44}^{(3)}}{C_{44}^{(2)}}\mathrm{c}_{3H} \\ 0 & 0 & 0 & 0 & \mathrm{c}_{3T} & \mathrm{s}_{3T} \\ 0 & 0 & 0 & 0 & -C_{44}^{(3)}\alpha^{(3)}\mathrm{s}_{3T} & C_{44}^{(3)}\alpha^{(3)}\mathrm{c}_{3T} \end{bmatrix} \begin{bmatrix} A_1 \\ B_1 \\ A_2 \\ B_2 \\ A_3 \\ B_3 \end{bmatrix} = \begin{bmatrix} W_B^{(1)} \\ S_{23B}^{(1)} \\ 0 \\ 0 \\ 0 \\ 0 \\ W_T^{(3)} \\ S_{23T}^{(3)} \end{bmatrix} \qquad (12)$$

It was denoted:

$$s_{2H}=\sin\left(\alpha^{(2)}y_H\right);\quad c_{2H}=\sin\left(\alpha^{(2)}y_L\right);$$
$$s_{3H}=\sin\left(\alpha^{(3)}y_H\right);\quad c_{3H}=\cos\left(\alpha^{(3)}y_H\right);$$
$$s_{2T}=\sin\left(\alpha^{(2)}y_{2T}\right);\quad c_{2T}=\sin\left(\alpha^{(2)}y_{2T}\right);$$
$$s_{3T}=\sin\left(\alpha^{(3)}y_{3T}\right);\quad c_{3T}=\cos\left(\alpha^{(3)}y_{3T}\right);$$

Selecting the stress free conditions for $y=y_{1B}$ and $y=y_{3T}$, from this system, one gets:

$$\begin{vmatrix} -s_{1B} & c_{1B} & 0 & 0 & 0 & 0 \\ c_{1L} & s_{1L} & -c_{2L} & -s_{2L} & 0 & 0 \\ -\frac{\alpha^{(1)}}{\alpha^{(2)}}s_{1L} & \frac{\alpha^{(1)}}{\alpha^{(2)}}c_{1L} & \frac{C_{44}^{(2)}}{C_{44}^{(1)}}s_{2L} & -\frac{C_{44}^{(2)}}{C_{44}^{(1)}}c_{2L} & 0 & 0 \\ 0 & 0 & c_{2H} & s_{2H} & -c_{3H} & -s_{3H} \\ 0 & 0 & -\frac{\alpha^{(2)}}{\alpha^{(3)}}s_{2H} & \frac{\alpha^{(2)}}{\alpha^{(3)}}c_{2H} & \frac{C_{44}^{(3)}}{C_{44}^{(2)}}s_{3H} & -\frac{C_{44}^{(3)}}{C_{44}^{(2)}}c_{3H} \\ 0 & 0 & 0 & 0 & -s_{3T} & c_{3T} \end{vmatrix}=0 \tag{13}$$

2.5. Three layers with springs interface

The spring interface between layers 2 and 3 (**Figure 1**) as defined by equation (4) can be written at the interface $y_{2T}=y_{3B}=y_T$ as $S_{23T}^{(2)}=R_S^{(2)}\left(W_B^{(3)}-W_T^{(2)}\right)$ or $S_{23T}^{(2)}=R_S^{(2)}\left(W_B^{(2)}-W_T^{(3)}\right)$ depending on the sign convention for the shear stress but there is no rule about the force sign in springs. In the case of two layers, the order in the difference of displacements is irrelevant for the dispersion curves, being just a change in signs for modal displacements. For the sake of uniformity, the following equations are deduced according to $S_{23T}^{(1)}=R_S^{(1)}\left(W_B^{(2)}-W_T^{(1)}\right)$ and $S_{23T}^{(2)}=R_S^{(2)}\left(W_B^{(3)}-W_T^{(2)}\right)$. The shear stress continuity at the interface between layers 2 and 3 is represented by the following equations:

$$S_{23T}^{(2)}=R_S^{(2)}\left(W_B^{(3)}-W_T^{(2)}\right)=C_{44}^{(2)}\alpha^{(2)}\left[-A_2\sin\left(\alpha^{(2)}y_H\right)+B_2\cos\left(\alpha^{(2)}y_H\right)\right]$$
$$S_{23L}^{(3)}=-R_S^{(2)}\left(W_B^{(3)}-W_T^{(2)}\right)=C_{44}^{(3)}\alpha^{(3)}\left[-A_3\sin\left(\alpha^{(3)}y_H\right)+B_3\cos\left(\alpha^{(3)}y_H\right)\right] \tag{14}$$

The full set of boundary conditions is:

$$\begin{bmatrix} c_{1B} & s_{1B} & 0 & 0 & 0 & 0 \\ -C_{44}^{(1)}\alpha^{(1)}s_{1B} & C_{44}^{(1)}\alpha^{(1)}c_{1B} & 0 & 0 & 0 & 0 \\ c\alpha_{1L}-R_S^{(1)}c_{1L} & -c\alpha_{1L}+R_S^{(1)}s_{1L} & R_S^{(1)}c_{2L} & R_S^{(1)}s_{2L} & 0 & 0 \\ R_S^{(1)}c_{1L} & R_S^{(1)}s_{1L} & -c\alpha_{2L}-R_S^{(1)}c_{2L} & c\alpha_{2L}-R_S^{(1)}s_{2L} & 0 & 0 \\ 0 & 0 & c\alpha_{2H}-R_S^{(2)}c_{2H} & -c\alpha_{2H}+R_S^{(2)}s_{2H} & R_S^{(2)}c_{3H} & R_S^{(2)}s_{3H} \\ 0 & 0 & R_S^{(2)}c_{2H} & R_S^{(2)}s_{2H} & -c\alpha_{3H}-R_S^{(2)}c_{3H} & c\alpha_{3H}-R_S^{(2)}s_{3H} \\ 0 & 0 & 0 & 0 & c_{3T} & s_{3T} \\ 0 & 0 & 0 & 0 & -C_{44}^{(3)}\alpha^{(3)}s_{3T} & C_{44}^{(3)}\alpha^{(3)}c_{3T} \end{bmatrix}\begin{bmatrix} A_1 \\ B_1 \\ A_2 \\ B_2 \\ A_3 \\ B_3 \end{bmatrix}=\begin{bmatrix} W_B^{(1)} \\ S_{23B}^{(1)} \\ 0 \\ 0 \\ 0 \\ 0 \\ W_T^{(3)} \\ S_{23T}^{(3)} \end{bmatrix} \tag{15}$$

The following notations were introduced:

$$csa_{2H}=C_{44}^{(2)}\alpha^{(2)}\sin\left(\alpha^{(2)}y_H\right);\quad cca_{2H}=C_{44}^{(2)}\alpha^{(2)}\cos\left(\alpha^{(2)}y_H\right);$$
$$csa_{3H}=C_{44}^{(3)}\alpha^{(3)}\sin\left(\alpha^{(3)}y_H\right);\quad cca_{3H}=C_{44}^{(3)}\alpha^{(3)}\cos\left(\alpha^{(3)}y_H\right);$$

For free surfaces at y_{1B} and y_{3T}, the dispersion equation is obtained by cancelling the determinant:

$$\begin{vmatrix} -s_{1B} & c_{1B} & 0 & 0 & 0 & 0 \\ c\alpha_{1L}-R_S^{(1)}c_{1L} & -c\alpha_{1L}+R_S^{(1)}s_{1L} & R_S^{(1)}c_{2L} & R_S^{(1)}s_{2L} & 0 & 0 \\ R_S^{(1)}c_{1L} & R_S^{(1)}s_{1L} & -c\alpha_{2L}-R_S^{(1)}c_{2L} & c\alpha_{2L}-R_S^{(1)}s_{2L} & 0 & 0 \\ 0 & 0 & c\alpha_{2H}-R_S^{(2)}c_{2H} & -c\alpha_{2H}+R_S^{(2)}s_{2H} & R_S^{(2)}c_{3H} & R_S^{(2)}s_{3H} \\ 0 & 0 & R_S^{(2)}c_{2H} & R_S^{(2)}s_{2H} & -c\alpha_{3H}-R_S^{(2)}c_{3H} & c\alpha_{3H}-R_S^{(2)}s_{3H} \\ 0 & 0 & 0 & 0 & -s_{3T} & c_{3T} \end{vmatrix}=0 \tag{16}$$

3. NUMERICAL EXAMPLES

An aluminum plate, of thickness $2h_1$=5 mm, mass density $\rho=2800\ kg/m^3$ and elastic constant $C_{44}=C_{55}=27\ GPa$ is considered, for which the dispersion curves obtained by solving the dispersion equation (6) are shown on Figure 2a. In the selected frequency range (0-2MHz) there are seven modes usually denoted SH_0 -SH_6.

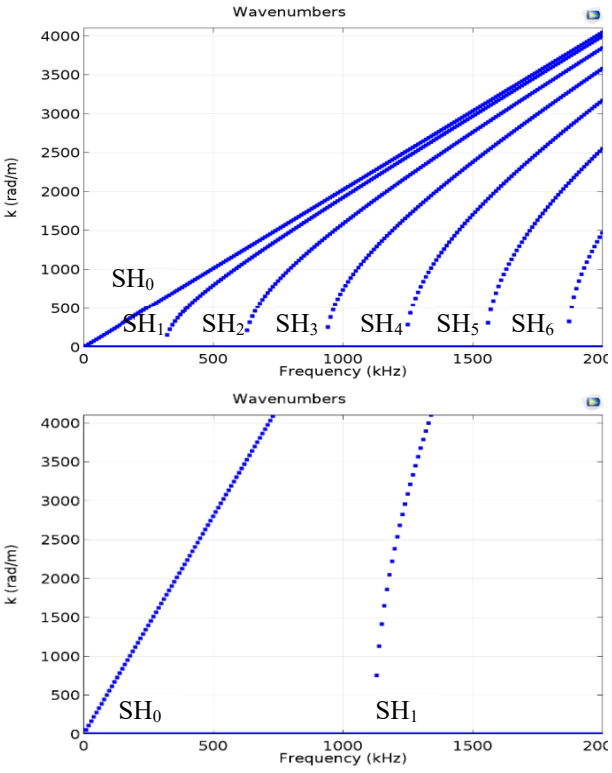

Figure 2. Dispersion curves: aluminum plate (a: up) and adhesive layer alone (b: down)

A layer of adhesive, of $2h_2 = 0.5$ mm thickness, with mass density $\rho^{(2)} = 1200\ kg/m^3$, elastic constants $C_{44}^{(2)} = C_{55}^{(2)} = 2\ GPa$, has been investigated and its dispersion curves are indicated on Figure 2b. There are two SH modes obtained by solving eq. (6) in this frequency range for the adhesive layer, having both surfaces stress-free.

A bi-layer made of the above mentioned aluminum plate, covered by the adhesive layer and then an three-layer sandwich made of two plates of aluminum (second plate having $2h_3 = 2$ mm), bonded by the mentioned adhesive are investigated solving the dispersion equations (8) and respectively (13). The dispersion curves are presented on Figure 3.

The interaction between the aluminum plate and the adhesive layer manifests through the progressive transition from the SH0 mode of the plate, towards a SH mode, which could be called SH quasi-Love (Q-Love) of the adhesive, in the frequency range 500 - 600 kHz (Figure 3a) and of specific modal shape (Figure 6). Such a transition exists also for the bonded plates (see Figure 3b, in the 900 -1100 kHz range).

The well-known phenomenon of modal doubling is clearly visible on Figure 3b, interlacing the modes of the aluminum plate and including SH_1 mode of the adhesive layer. Many of these aspects have been discussed in the cited references.

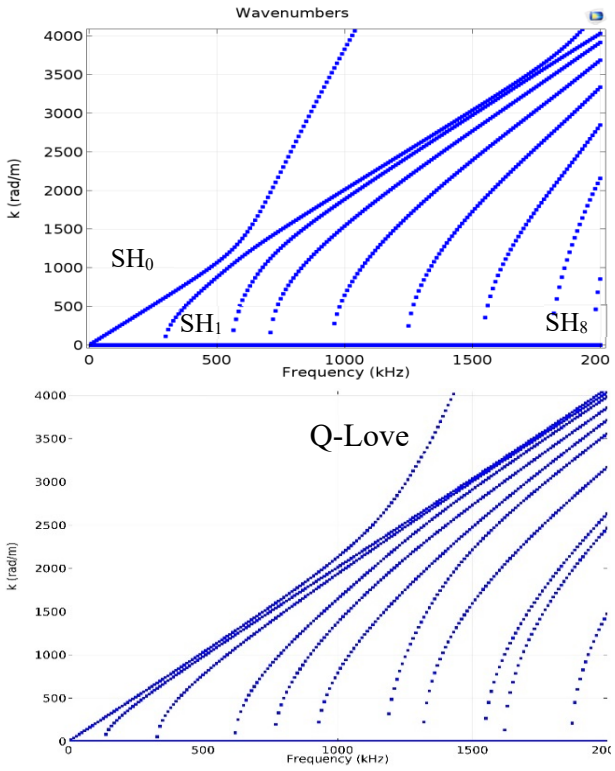

Figure 3. Dispersion curves for a plate with a layer of adhesive (a: up) and two plates of aluminum perfectly bonded by an adhesive layer (b: down).

3.1. Spring stiffness influence

The three-layer made of two identical aluminum plates, defined by the parameters mentioned in the previous paragraph, are investigated from the point of view of springs stiffness influence.

In order to focus on the spring model limitations, both interfaces will be considered in this paragraph to be of identical stiffnesses $R_S^{(1)} = R_S^{(2)}$.

On Figure 4 are presented the dispersion curves for decreasing adhesion strength, represented by decreasing spring constants. Certainly, if $R_S \to \infty$, the adhesion is perfect and the dispersion curves are those shown on Figure 4b. The presence of the adhesive between the two aluminum plates, transforms the SH_0 mode at frequencies above 1 MHz, into a SH Q-Love mode. As R_S decreases, this transition occurs at higher frequencies, the adhesive layer being less connected to the metallic plates.

Important is the R_S value, for which noticeable differences begin to occur. Small differences can be identified for $R_S = 10^{15}$ N/m (Figure 4).

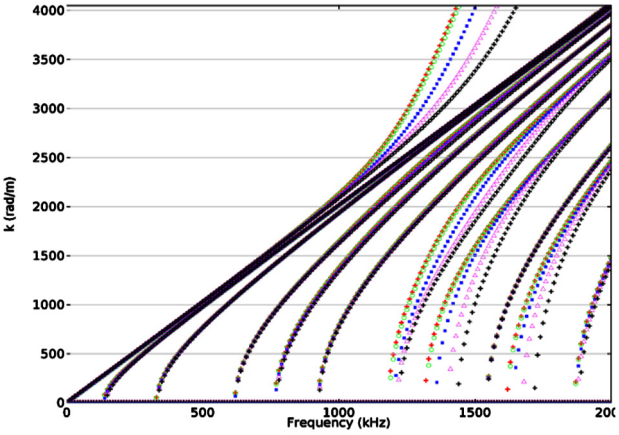

Figure 4. Dispersion curves for two plates of aluminum bonded by an adhesive layer: perfect adhesion (+), $R_S = 10^{15}$ (o), $R_S = 10^{14}$(·), $R_S = 5\cdot10^{13}$(Δ), $R_S = 3.5\cdot10^{13}$(+)

This order of magnitude can be considered in the investigated case, as a limit value, below which a bonding degradation can be identified [2]. As can be seen on the same figure, for $R_S = 10^{14}$ N/m, the dispersion curves for several modes (SH_6 .. SH_9) are considerably different than in the perfect adhesion case. Reducing the spring stiffness to $R_S = 5\cdot10^{13}$ N/m, the dispersion curves continue this trend, but for values below $R_S = 3.5\cdot10^{13}$ N/m wrong solutions will appear, with impossible wavenumbers, having large values for a null frequency.

Consequently, the spring model provides acceptable results for R_S between $3.5\cdot10^{13}$ N/m and 10^{15} N/m, above which the dispersion curves correspond to the perfect contact. Below RS $= 3.5\cdot10^{13}$ N/m, the three-layer using this model can be considered as inadequate.

3.2. Springs force sense influence

For the investigated three-layer structure there are two interfaces modeled by springs, connecting the adhesive layer and the two plates, according to eq. (4) and (9).

However, the distributed forces produced in the springs can be positive (traction) or negative (compression) depending on the sign of the displacements differences between the two ends of the spring layers, which in this case are the displacements of the connected elastic layers.

In the previous paragraphs, the shear forces produced by the springs are proportional to the following differences of displacements:

$$\begin{aligned} S_{23T}^{(1)} &= R_S^{(1)}\left(W_B^{(2)} - W_T^{(1)}\right) \\ S_{23T}^{(2)} &= R_S^{(2)}\left(W_B^{(3)} - W_T^{(2)}\right) \end{aligned} . \qquad (17)$$

These formulas refer to the shear stresses on the "top" surface of layer (1) and (2). Certainly, the springs equilibrium requires opposite signs for the stresses on the "bottom" surfaces of layers (2) and (3) (Figure **5**).

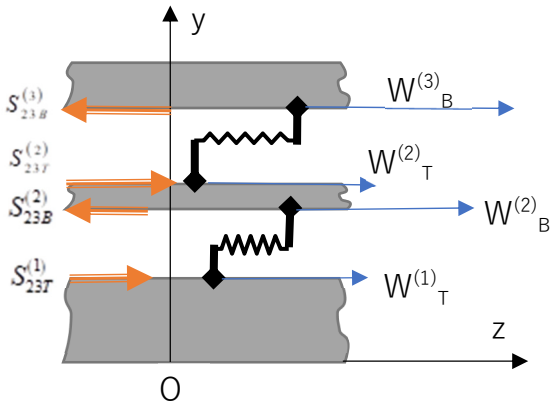

Figure 5. Positive shear stresses and spring producing tractions

The signs of the shear stresses can be considered as opposite if the Oy axis is in the opposite sense. The forces in the two spring's interfaces can thus be chosen in the opposite sense:

$$\begin{aligned} S_{23T}^{(1)} &= -R_S^{(1)}\left(W_B^{(2)} - W_T^{(1)}\right) \\ S_{23T}^{(2)} &= -R_S^{(2)}\left(W_B^{(3)} - W_T^{(2)}\right) \end{aligned} . \qquad (18)$$

Displacements for mode SHQ-Love at 1.2 MHz are shown on Figure 6 for the perfect contact and for springs defined according to equations (17) and (18). Between y = 0 and 5 mm are the displacements in the 5mm thick Aluminum plate, followed by those in the 0.5mm thick adhesive, then in the 2mm thick Aluminum plate.

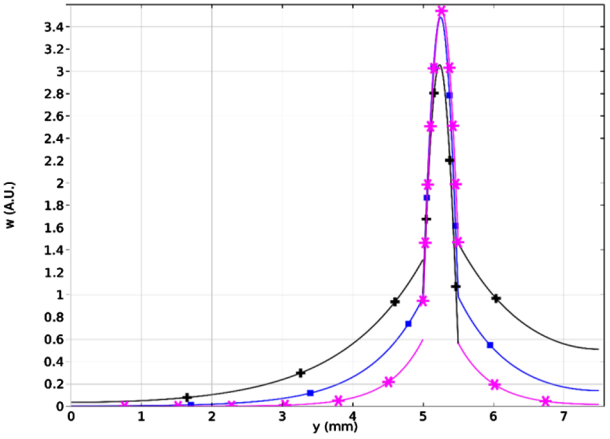

Figure 6. Displacements of the SHQ-Love mode at 1.2MHz. Perfect adhesion (■), springs defined by **(17)** (+) and springs defined by **(18)** (*).

Using equations (17), the displacements jump is negative between layer 1 and 2, but positive between layer 2 and 3. The shear stresses are accordingly negative and respectively positive in formulas (18).

Overall, the displacements in the adhesive layer suffer a negative jump in the presence of springs, compared to the perfect adhesion continuity condition. If one is using equations (18), the displacements jump is positive between layer 1 and 2, and negative between layer 2 and 3.

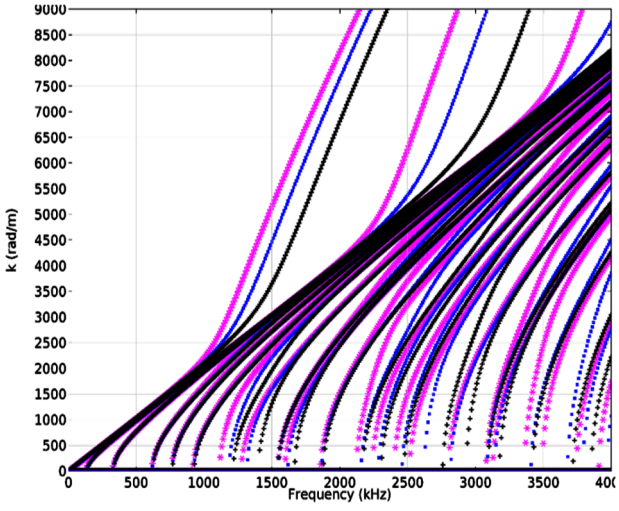

Figure 7. Dispersion curves for the three-layer with $R_{S1} = 1 \cdot 10^{13}$ N/m, $R_{S1} = 3.5 \cdot 10^{13}$ N/m, springs defined by (17) (+) and springs defined by (18) (*). For comparison, perfect adhesion (■).

The dispersion curves are recomputed with this sign convention (Figure 7) then superposed on those with the correct sign and those valid for perfect

adhesion. The dispersion curves have opposite variations compared to the perfect adhesion case. These variations are visible, mostly for the SHQ-Love modes, but also for higher order SH modes.

Consequently, the sign of the forces in the springs plays an essential role in the correct assessment of the dispersion curves.

4. CONCLUSIONS

The shear springs interfaces are used to model the adhesion quality, by changing the elastic spring constants. Detailed equations for the SH waves have been deduced for a single layer, a bi-layer and then a three-layer case, in the perfect adhesion case and in the spring interface case. An interface mode, with displacements mostly in the adhesive layer and decaying in the aluminum plates, is named SH Quasi-Love and is presented as deriving from SH0 mode at higher frequencies, having specific modal displacements. This mode is hard to detect since only very weak displacements exist at the free surfaces.

It has been proven that a good adhesion can be represented by $R_S = 10^{15}$ N/m, whereas the weakest adhesion was modeled using $R_S = 3.5 \cdot 10^{13}$ N/m. Unfortunately, such values required by this spring model, are difficult to interpret, being incompatible with the elasticity constants of the involved materials. The choice of signs in the shear forces definitions can be a critical issue, since completely different dispersion curves evolutions are obtained by simply changing the elastic forces signs.

As a general conclusion, this simple spring model has some shortcomings, requiring thus a careful use, as indicated in this paper.

REFERENCES

[1] Jones J.P., Whittier J.S., Waves at a flexibly bonded interface, *J. Appl. Mech.*, Vol. 34, No. 4, 1967, pp. 905-909.

[2] Gauthier C. et al., Lamb waves characterization of adhesion levels in aluminum/epoxy bi-layers with different cohesive and adhesive properties, *International Journal of Adhesion and Adhesives*, Vol. 74, 2017.

[3] Leduc D., El-Kettani M.E-C., Attar L., Predoi M.V., Pareige P., Bonding characterization of a three-layer metal-adhesive-metal using shear horizontal modes of close dispersion curves, *Acta Acustica united with Acustica*, Vol. 103, No. 6, 2017.

[4] Lowe M.J.S., Challis R.E., Chan C.W., The transmission of Lamb modes across bonded lap joints, *J. Acoust. Soc. Am.*, Vol. 107, No. 3, 2000, pp. 1333-1345.

[5] Heller K., L. Jacobs J., Qu J., Characterization of adhesive bond properties using Lamb waves, *NDT&E Int.*, Vol. 33, 2000, pp. 555–563.

[6] Hosten B., Castaings M., Finite elements methods for modeling the guided waves, *J. Acoust. Soc. Am.*, Vol. 117, No. 3, 2005, pp. 1108–1113.